

Band engineering of double-wall Mo-based hybrid nanotubes

Lei Tao(陶蕾), Yu-Yang Zhang(张余洋), Jiatao Sun(孙家涛), Shixuan Du(杜世萱), Hong-Jun Gao(高鸿钧)

Citation: Chin. Phys. B . 2018, 27(7): 076104. **doi:** 10.1088/1674-1056/27/7/076104

Journal homepage: http://cpb.iphy.ac.cn; http://iopscience.iop.org/cpb

What follows is a list of articles you may be interested in

Novel conductance step in carbon nanotube with wing-like zigzag graphene nanoribbons

Hong Liu(刘红)

Chin. Phys. B . 2017, 26(11): 116101. **doi:** 10.1088/1674-1056/26/11/116101

Stable single helical C- and I-chains inside single-walled carbon nanotubes

Z Yao(姚震), C J Liu(刘春见), Y Li(李义), X D Jing(敬晓丹), F S Meng(孟凡顺), S P Zheng(郑士鹏), X Zhao(赵星), J H Li(李久会), Z Y Qiu(邱忠媛), Q Yuan(袁泉), W X Wang(王文新), L Bi(毕磊), H Liu(刘辉), Y P Zhang(张玉璞), B B Liu(刘冰冰)

Chin. Phys. B . 2016, 25(9): 096105. **doi:** 10.1088/1674-1056/25/9/096105

Structural transitions of SWNT filled with C_{60} under high pressure

Yong-gang Zou(邹永刚), Li Xu(徐莉), Kun Tian(田锟), He Zhang(张贺), Xiao-hui Ma(马晓辉), Ming-guang Yao(姚明光)

Chin. Phys. B . 2016, 25(5): 056101. **doi:** 10.1088/1674-1056/25/5/056101

Channeling of fast ions through the bent carbon nanotubes: The extended two-fluid hydrodynamic model

Lazar Karbunar, Duško Borka, Ivan Radović, Zoran L Mišković

Chin. Phys. B . 2016, 25(4): 046106. **doi:** 10.1088/1674-1056/25/4/046106

Electron irradiation-induced change of structure and damage mechanisms in multi-walled carbon nanotubes

Yang Jian-Qun, Li Xing-Ji, Liu Chao-Ming, Ma Guo-Liang, Gao Feng

Chin. Phys. B . 2015, 24(11): 116103. **doi:** 10.1088/1674-1056/24/11/116103

Band engineering of double-wall Mo-based hybrid nanotubes*

Lei Tao(陶蕾)[1,2], Yu-Yang Zhang(张余洋)[1,2,3], Jiatao Sun(孙家涛)[1,2], Shixuan Du(杜世萱)[1,2,3,†], and Hong-Jun Gao(高鸿钧)[1,2,3]

[1] *Institute of Physics, Chinese Academy of Sciences, Beijing* 100190, *China*
[2] *University of Chinese Academy of Sciences, Beijing* 100190, *China*
[3] *CAS Center for Excellence in Topological Quantum Computation, Chinese Academy of Sciences, Beijing* 100190, *China*

(Received 18 April 2018; revised manuscript received 24 April 2018; published online 25 June 2018)

Hybrid transition-metal dichalcogenides (TMDs) with different chalcogens on each side (X-TM-Y) have attracted attention because of their unique properties. Nanotubes based on hybrid TMD materials have advantages in flexibility over conventional TMD nanotubes. Here we predict the wide band gap tunability of hybrid TMD double-wall nanotubes (DWNTs) from metal to semiconductor. Using density-function theory (DFT) with HSE06 hybrid functional, we find that the electronic property of X-Mo-Y DWNTs (X = O and S, inside a tube; Y = S and Se, outside a tube) depends both on electronegativity difference and diameter difference. If there is no difference in electron negativity between inner atoms (X) of outer tube and outer atoms (Y) of inner tube, the band gap of DWNTs is the same as that of the inner one. If there is a significant electronegativity difference, the electronic property of the DWNTs ranges from metallic to semiconducting, depending on the diameter differences. Our results provide alternative ways for the band gap engineering of TMD nanotubes.

Keywords: band engineering, nanotube, hybrid transition metal dichalcogenides, first-principle calculations

PACS: 61.46.Fg, 73.20.At, 73.22.–f **DOI:** 10.1088/1674-1056/27/7/076104

1. Introduction

Nanotubes which can be formed by rolling up two-dimensional materials, such as graphene and transition-metal dichalcogenides (TMDs), have attracted a great deal of attention due to their distinct physical and chemical properties.[1–5] Nanotubes based on TMDs are semiconductors with wide applications including field-effect transistors,[6–8] photodetectors,[9] and solid lubricants.[10] Similar to carbon nanotubes (CNTs), the properties of TMD nanotubes, such as band gap,[11,12] mechanic property,[13,14] carrier mobility,[15] and optical conductivity,[16] are predicted to be diameter-dependent. Because the bending energy is proportional to the effective thickness to the power three,[17] it is hard to roll TMD nanotubes with small diameters. Theoretical calculations predicted that the smallest diameter of MoS_2 nanotube is larger than 6 nm,[18] which was confirmed by experimental observations.[19] Thus, the band gap tunability of fabricated TMD nanotubes is limited as a result of the large diameter.[8]

Recently, hybrid TMD materials with different chalcogen on each side of the sandwich structure, for example, Janus S-Mo-Se, have been fabricated.[20,21] Because of the different chalcogens on each side, hybrid TMD materials tend to bend to release the intrinsic strain. Thus, hybrid TMDs are believed to be good candidates to form nanotubes with a smaller diameter (less than 2 nm).[22] There are some calculations based on density-function theory (DFT) about hybrid TMD single-wall nanotubes (SWNTs), such as S-Mo-Te nanotube and S-Mo-Se nanotube.[22,23] Band structure of hybrid S-Mo-Te nanotube is similar to that of the conventional TMD nanotube, which is tunable from 0 to 1.5 eV. The maximum band gap is attributed to the fully released strain when the S-Mo-Te nanotube has the particular diameter.[22] In the hybrid S-Mo-Se armchair nanotube, the band gap ranges from 0.4 eV to 1.6 eV with an indirect-direct band gap transition.[23] However, those calculations based on Perdew–Burke–Ernzerhof function (PBE) underestimate the band gaps, especially for small nanotubes.[15] The accurate band gaps of small TMD SWNTs are still unknown.

In this paper, we first calculated the band gaps of several TMD SWNTs using HSE06 hybrid functional, which is believed to give a reliable band structure.[24,25] All the SWNTs are semiconductors. The band gap is larger than 0.5 eV when the diameter of the nanotube is as small as 1 nm. Then we constructed the double-wall nanotubes (DWNTs) using hybrid X-Mo-Y SWNTs with different components (X = O and S, inside a tube; Y = S and Se, outside a tube). Further DFT calculations show that the DWNTs are either metallic or semiconducting with a band gap ranging from zero to that of the inner

*Project supported by the National Key Research and Development Program of China (Grant No. 2016YFA0202300), the National Natural Science Foundation of China (Grant No. 61390501), the National Basic Research Program of China (Grant No. 2013CBA01600), Strategic Priority Research Program (B) of Chinese Academy of Sciences (Grant Nos. XDPB0601 and XDPB08-1), the CAS Pioneer Hundred Talents Program, and Beijing Nova Program, China (Grant No. Z181100006218023).

†Corresponding author. E-mail: sxdu@iphy.ac.cn

© 2018 Chinese Physical Society and IOP Publishing Ltd

nanotube. When there is no electronegativity difference between inner atoms of the outer tube and outer atoms of the inner tube, the combination is semiconducting. The band edges of the DWNTs are contributed by the inner tube. If there is a significant electronegativity difference between the two tubes, the electronic properties of DWNTs range from metallic to semiconducting depending on the diameter difference. When the diameter difference is small, there is a significant electron transfer between the two tubes, leading to metallic DWNTs. When the diameter difference increases, the interlayer interaction decreases and DWNTs remain semiconductors. For the case of two O-Mo-S nanotubes, the critical distance of semiconducting-to-metallic transition is 5.3 Å. Our results demonstrate that the band gaps of hybrid TMD DWNTs are tunable in a wide range from metallic to semiconducting and may provide contributions to electronic devices.

2. Method

DFT calculations were performed by using the Vienna *ab initio* simulation package (VASP)[26] with the projected augmented wave (PAW) method.[27] The wave functions were expanded in a plane-wave basis set with a 400 eV energy-cutoff. Structural optimizations were carried out using Perdew–Burke–Ernzerhof (PBE) exchange and correlation function.[28] The distance between two adjacent nanotubes was larger than 10 Å. Net force on each atom was smaller than 0.02 eV/Å, with a fully converged k-point sampling in the first Brillion zone. Band structure calculations were performed with a more accurate and reliable Heyd–Scouseria–Ernzerhof (HSE06) scheme.[29,30]

3. Results and discussion

Figure 1(a) shows the atomic structure of a flat hybrid X-Mo-Y material, which has different atoms on each side of the sandwich structure. X is the element with a smaller atomic radius, and Y is the element with a larger atomic radius. Hybrid X-Mo-Y nanotubes can be rolled up by hybrid X-Mo-Y materials, with the large atoms (Y) outside and the small atoms (X) inside. In this work, the inner atoms (X) are O and S, and the outer atoms (Y) are S and Se. Similar to CNTs, the chiral vectors of TMD nanotubes are also defined by the unit vectors. A zigzag nanotube (ZNT) is defined by the chiral vector (n, 0), and an armchair nanotube (ANT) is defined by the chiral vector (n,n).

For a hybrid X-Mo-Y nanotube, a small nanotube is more favorable when there is a large atomic size difference between the atoms X and Y on the two sides of the nanotube.[22] The empirical van der Waals radii are 1.71 Å, 2.06 Å, and 2.18 Å for O, S, and Se, respectively.[31] The atomic size difference between O and S/Se is larger than that between S and Se, resulting in a smaller nanotube when there are O atoms inside and S/Se atoms outside. The internal diameters and the external diameters of each single-wall hybrid X-Mo-Y nanotube are listed in Table 1. The smallest external diameters of the armchair nanotubes are 0.99 nm for the O-Mo-S (4,4) nanotube.

Electronic properties of nanotubes depend both on diameter and chirality. It is worth noting that the band gaps of TMD nanotubes have been underestimated in previous calculations due to the choice of PBE functional, especially for small nanotubes.[15,22] We use both PBE and the more accurate HSE06 hybrid functional to examine the band gaps, which are shown in Table 2.

The band gap increases when the diameter increases. By using the HSE06 hybrid functional, the band gap is 0.51 eV for the smallest O-Mo-S (4, 4) nanotube, while calculations based on the PBE functional reveal that the O-Mo-S (4, 4) nanotube is metallic.

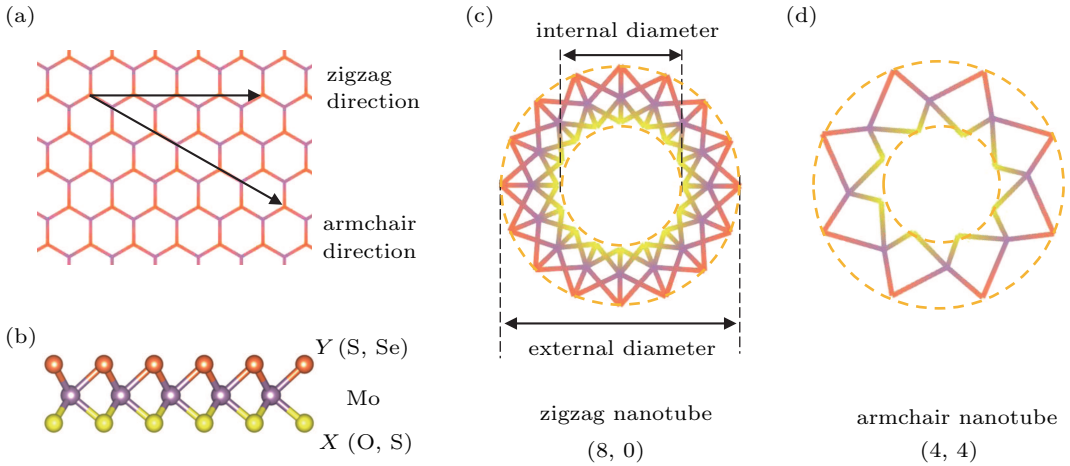


Fig. 1. (color online) A schematic of hybrid X-Mo-Y nanotubes. (a) The top view of a flat hybrid X-Mo-Y material. The directions of zigzag and armchair are marked by black arrows. (b) Side view of a flat hybrid X-Mo-Y material. Different atoms at each side are labeled as X and Y. X is the element with a smaller atomic radius (O or S), and Y is the element with a larger atomic radius (S or Se). Side view of (c) a zigzag single-wall hybrid X-Mo-Y (8, 0) nanotube and (d) an armchair single-wall hybrid X-Mo-Y (4, 0) nanotube.

Table 1. Internal diameter and external diameter of all X-Mo-Y nanotubes.

Diameter/Å		O-Mo-S		O-Mo-Se		S-Mo-Se	
		Internal diameter	External diameter	Internal diameter	External diameter	Internal diameter	External diameter
Armchair	(4,4)	4.67	9.90	4.67	10.11	5.35	11.09
	(7,7)	9.20	14.71	9.30	15.04	10.13	16.36
	(10,10)	14.08	19.63	14.27	20.05	15.24	21.59
Zigzag	(8,0)	6.04	11.43	6.16	11.77	6.76	12.72
	(14,0)	11.11	16.65	11.25	17.01	12.31	18.58
	(20,0)	16.52	22.11	16.88	22.68	18.17	24.54

Table 2. Band gaps of X-Mo-Y (X = O and S, inside a tube; Y = S and Se, outside a tube) nanotubes using PBE and HSE06.

Band gap/eV		O-Mo-S		O-Mo-Se		S-Mo-Se	
		PBE	HSE06	PBE	HSE06	PBE	HSE06
Armchair	(4,4)	0.00	0.51	0.07	0.67	0.00	0.58
	(7,7)	0.80	1.49	0.80	1.53	0.79	1.42
	(10,10)	0.97	1.71	0.90	1.62	1.25	1.90
Zigzag	(8,0)	0.27	0.68	0.30	0.72	0.34	0.71
	(14,0)	0.76	1.25	0.73	1.23	0.90	1.46
	(20,0)	1.08	1.65	0.90	1.41	1.28	1.78

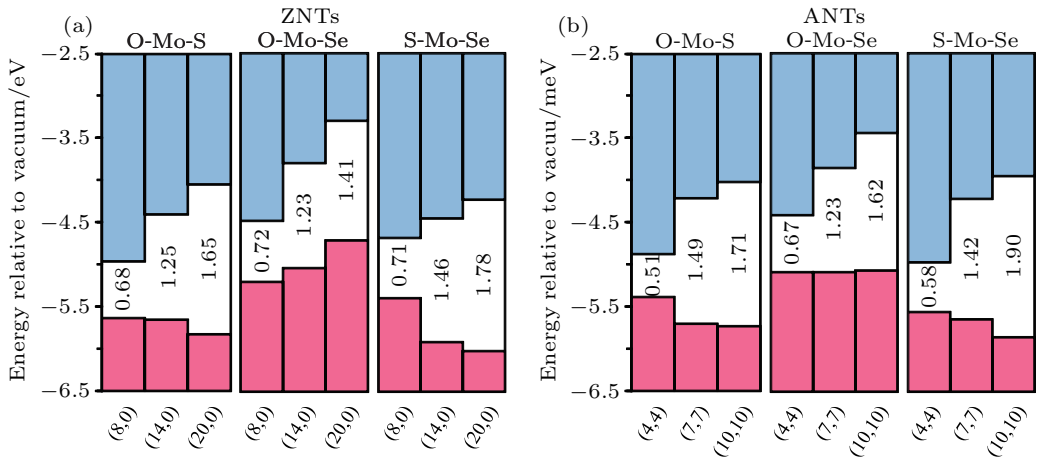


Fig. 2. (color online) Band gapes and band edge positions of single-wall hybrid X-Mo-Y nanotubes (O-Mo-S, O-Mo-Se and S-Mo-Se) with different sizes: (a) ZNTs and (b) ANTs.

In order to tune the band gap of hybrid X-Mo-Y nanotubes in a wide range, we investigate the hybrid X-Mo-Y DWNTs system. Hybrid X-Mo-Y DWNTs are combined with two hybrid X-Mo-Y SWNTs of different sizes. We choose DWNTs (8, 0)@(20, 0) and (4, 4)@(10, 10). The DWNT (8, 0)@(20, 0) consists of a hybrid ZNT (8, 0) inside and a hybrid ZNT (20, 0) outside, and the DWNT (4, 4)@(10, 10) consists of a hybrid ANT (4, 4) inside and a hybrid ANT (10, 10) outside. There is a lattice mismatch between the outer and inner tubes and in the calculations we use the lattice constant of the smaller one (inner tube), because axial tension has more significant influence on the band structure than compression in TMD nanotubes.[32]

We investigate the influence of electronegativity difference on the properties of DWNTs. Figures 3(b) and 3(g) show the band structures of the DWNT O-Mo-S(8, 0)@S-Mo-Se(20, 0) and the DWNT O-Mo-S(4, 4)@S-Mo-Se(10, 10). In both cases, there is no difference in electron negativity between the inner atoms of the outer tube and the outer atoms of the inner tube. The diameter difference between the internal diameter of the outer tube and the external diameter of the inner tube is 4.1 Å for the DWNT O-Mo-S(8, 0)@S-Mo-Se(20, 0) and 3.1 Å for the DWNT O-Mo-S(4, 4)@S-Mo-Se(10, 10). We find that both the zigzag and armchair DWNTs are semiconducting. The band structure of DWNTs is a superposition of the bands of the inner nanotube and outer nanotube, and the band structure of each single-wall hybrid X-Mo-Y nanotube remains. The band gaps of both zigzag and armchair DWNTs are equal to those of the inner tubes. The zigzag DWNT has direct band gaps and the armchair DWNT has indirect band gaps. The highest valence band and the lowest conduction band in both of the DWNTs are contributed by the inner tube (marked by blue lines), which is in consistent with the band edge positions in Figs. 2(a) and 2(b).

If there is a significant electronegativity difference be-

tween the inner atoms of the outer tube and the outer atoms of the inner tube, the electronic property of DWNTs is determined by the diameter difference. Figures 3(c) and 3(d) show the band structures of zigzag DWNTs O-Mo-S(8, 0)@O-Mo-Se(20, 0) and O-Mo-S(8, 0)@O-Mo-S(20, 0). In those DWNTs, the inner atoms of the outer tube are O and the outer atoms of the inner tube are S and Se. The difference between the internal diameter of the outer tube and the external diameter of the inner tube is 3.0 Å for O-Mo-S@O-Mo-S, and 3.9 Å for O-Mo-S@O-Mo-Se. Both of these zigzag DWNTs are metallic. Figures 3(h) and 3(i) show the band structures of armchair DWNTs O-Mo-S(4, 4)@O-Mo-Se(10, 10) and O-Mo-S(4, 4)@O-Mo-S(10, 10). The armchair DWNTs are also metallic. The diameter difference is 2.3 Å for O-Mo-S@O-Mo-S and 2.6 Å for O-Mo-S@O-Mo-Se. The diameter of the inner tube is smaller than that of the single-wall hybrid *X*-Mo-*Y* nanotube because of the interlayer interaction in DWNTs.

In both zigzag and armchair DWNTs, the energy bands of the inner tube are shifted to higher energy levels. The valence band of the inner tubes (marked by red lines) and the conduction band of the outer tubes (marked by blue lines) are both partially occupied, leading to metallic DWNTs. The results indicate that the electronic properties of DWNTs are dominated by the electronegativity difference between the inner element of the outer tubes and the outer element of the inner tubes. The outmost atoms of the outer tubes have no significant influence on the electronic properties.

Figures 3(e) and 3(j) show the band structures of DWNTs O-Mo-S(8, 0)@O-Mo-S(28, 0) and O-Mo-S(4, 4)@O-Mo-S(14, 14). The diameter difference is 6.5 Å for DWNT O-Mo-S(8, 0)@O-Mo-S(28, 0), and 5.3 Å for DWNT O-Mo-S(4, 4)@O-Mo-S(14, 14). When the diameter difference of the two tubes increases, the DWNTs restore to semiconducting because the interlayer interaction decreases. The zigzag DWNTs have a direct band gap and the armchair DWNTs have an indirect band gap, which are the same as each single-wall hybrid *X*-Mo-*Y* nanotube in the combinations.

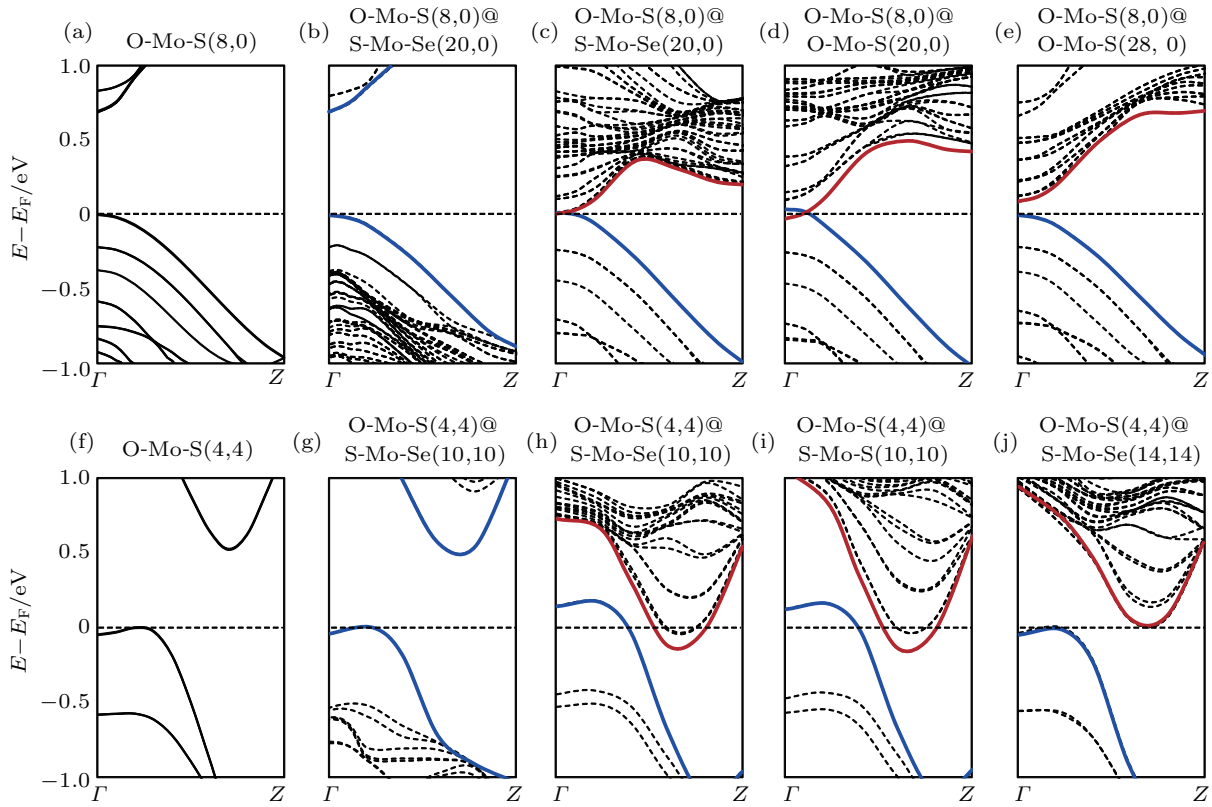


Fig. 3. (color online) Band structures of hybrid *X*-Mo-*Y* nanotubes. (a) Zigzag hybrid SWNT O-Mo-S (8, 0). (b)–(d) DWNTs consisted of O-Mo-S (8, 0) and hybrid *X*-Mo-*Y* (20, 0) (*X*-Mo-*Y* = S-Mo-Se, O-Mo-Se, O-Mo-S) nanotubes. (e) DWNTs O-Mo-S(8, 0)@O-Mo-S(28, 0). (f) Armchair hybrid SWNT O-Mo-S (4, 4). (g)–(i) DWNTs consisted of O-Mo-S (4, 4) and hybrid *X*-Mo-*Y* (10,10) (*X*-Mo-*Y* = S-Mo-Se, O-Mo-Se, O-Mo-S) nanotubes. (j) O-Mo-S(4, 4)@O-Mo-S(14, 14). The blue lines are contributed by the inner nanotubes and the red lines are contributed by the outer nanotubes.

The band gap is 0.12 eV in Fig. 3(e), and 0.05 eV in Fig. 3(j). The shifted energy bands also keep the feature of the freestanding ones. The highest valence band is contributed by the inner tube and the lowest conduction band is contributed by the outer tube. The results, together with Figs. 3(d) and 3(i), show that the electronic properties of DWNTs are also determined by the diameter difference. For DWNTs O-Mo-S@O-Mo-Se, when the distance between the two tubes is smaller than 5.3 Å, the DWNTs are metallic. When the diameter difference is larger than 5.3 Å, the DWNTs become semicon-

ducting with a band gap smaller than that of the inner tube. Compared to the band edge positions in Figs. 2(a) and 2(b), the energy level shifts are interpreted in terms of interlayer interaction between the two tubes, which plays the crucial role in the band structures of the DWNTs.

To further understand the semiconducting-to-metallic transition, we plot the electron density difference for the two metallic DWNTs O-Mo-S(8, 0)@O-Mo-S(20, 0) and O-Mo-S(4, 4)@O-Mo-S(10, 10) (Figs. 4(a) and 4(c)). The electron density difference is widely used to analyze the interaction between two systems,[33] and is defined as $\Delta\rho = \rho(\text{DWNTs}) - \rho(\text{inner nanotube}) - \rho(\text{outer nanotube})$. The red and green areas represent electron accumulation and electron depletion regions, respectively. Significantly, there is an electron transfer from the inner tube to the outer tube in the DWNT O-Mo-S(8, 0)@O-Mo-S(20, 0) and the DWNT O-Mo-S(4, 4)@O-Mo-S(10, 10).

Figures 4(b)–4(d) and 4(f)–4(h) are the integrals of electron density difference along the radical direction in different DWNTs. The black dash lines are marked in the positions of the inner atoms of the outer tubes and the outer atoms of the inner tubes. Electron transfer in Figs. 4(b) and 4(f) is more significant than that in Figs. 4(c) and Fig. 4(g), indicating a stronger interlayer interaction in the DWNT O-Mo-S@O-Mo-S than that in the DWNT O-Mo-S@S-Mo-Se, which is consistent with the results in Figs. 3(b), 3(d), 3(g), and 3(i). Because of the increased diameter difference, there is no significant electron transfer between the two tubes in Figs. 4(d) and 4(h), resulting in the semiconducting DWNTs O-Mo-S(8, 0)@O-Mo-S(28, 0) and O-Mo-S(4, 4)@O-Mo-S(14, 14).

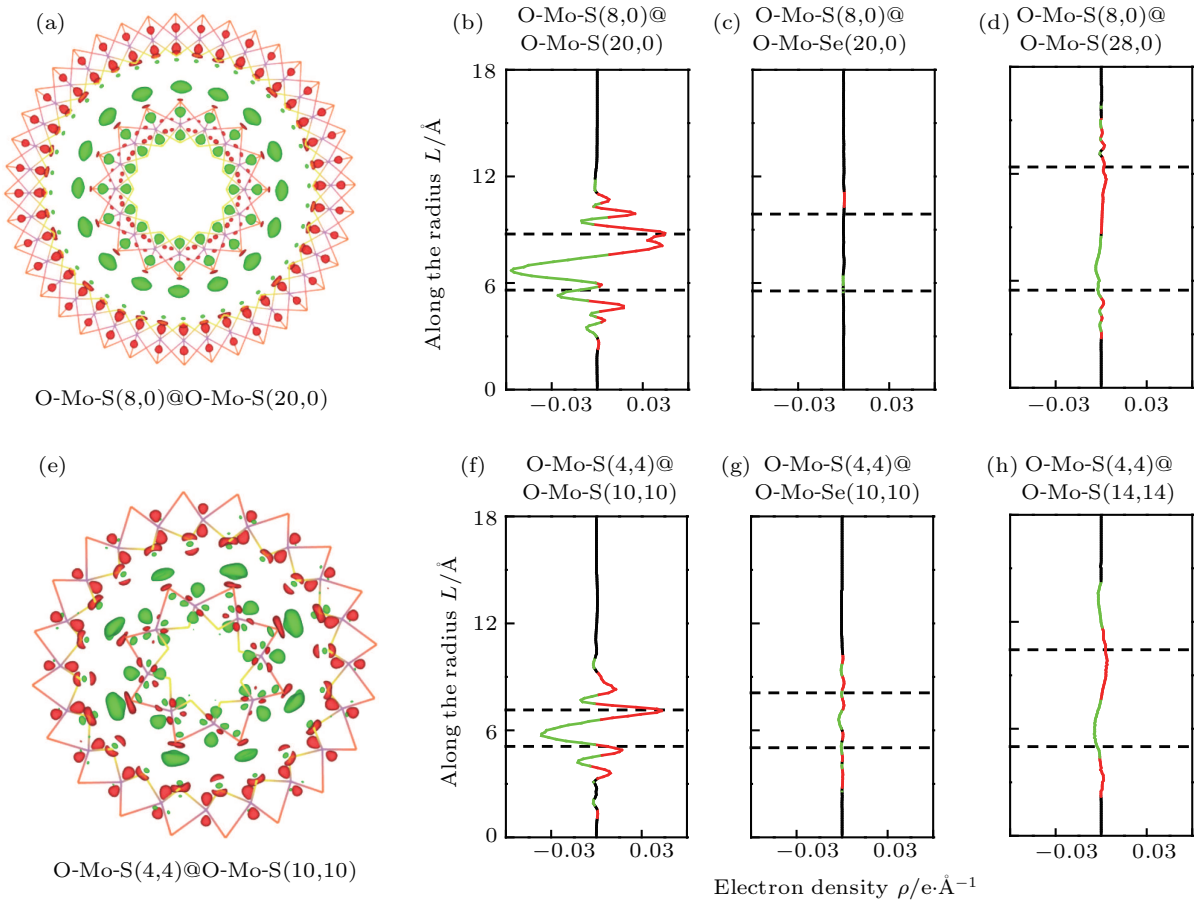


Fig. 4. (color online) Electron redistribution in hybrid *X*-Mo-*Y* DWNTs. (a) and (e) Electron density difference for the DWNT O-Mo-S(8, 0)@O-Mo-S(20, 0) and the DWNT O-Mo-S(4, 4)@O-Mo-S(10, 10). The red and green areas represent electron accumulation and electron depletion regions, respectively. The isosurface is 0.001 e/Bohr^3. (b)–(d) Integrals of electron density difference along the radius direction in three zigzag DWNTs. (f)–(h) Integrals of electron density difference along the radius direction in armchair DWNTs. The black dash lines refer to the positions of the inner atoms of the outer tubes and the outer atoms of the inner tubes.

4. Conclusion

In summary, we investigate the tunability of hybrid *X*-Mo-*Y* SWNTs and DWNTs. We demonstrate that *X*-Mo-*Y* SWNTs are all semiconductors with band gaps larger than 0.5 eV. For hybrid *X*-Mo-*Y* DWNTs, the electronic properties are tunable in a wide range from metallic to semiconducting, which depends on both electronegativity difference and diameter difference. Our results show the influences of the interlayer interaction on the band structures of hybrid *X*-Mo-*Y* DWNTs, and provide alternative ways to tune the band gaps of TMD nanotubes.

Acknowledgments

A portion of the research was performed in CAS Key Laboratory of Vacuum Physics. Computational resources were provided by the National Supercomputing Center in Tianjin.

References

[1] Barros E B, Jorio A, Samsonidze G G, Capaz R B, Souza Filho A G, Mendes Filho J, Dresselhaus G and Dresselhaus M S 2006 *Phys. Rep.* **431** 261
[2] Guo W, Hu Y B, Zhang Y Y, Du S X and Gao H J 2009 *Chin. Phys. B* **18** 2502
[3] Min Z and Jun S 2014 *Chin. Phys. B* **23** 017301
[4] Dai X, Zhou Y, Li J, Zhang L, Zhao Z and Li H 2017 *Chin. Phys. B* **26** 087310
[5] Xiao Z, Fan M, Ju T and Bing Y 2012 *Acta Phys. Sin.* **61** 156101 (in Chinese)
[6] Levi R, Bitton O, Leitus G, Tenne R and Joselevich E 2013 *Nano Lett.* **13** 3736
[7] Fathipour S, Remskar M, Varlec A, Ajoy A, Yan R, Vishwanath S, Rouvimov S, Hwang W S, Xing H G, Jena D and Seabaugh A 2015 *Appl. Phy. Lett.* **106** 022114
[8] Strojnik M, Kovic A, Mrzel A, Buh J, Strle J and Mihailovic D 2014 *AIP Advances* **4** 097114
[9] Zhang C, Wang S, Yang L, Liu Y, Xu T, Ning Z, Zak A, Zhang Z, Tenne R and Chen Q 2012 *Appl. Phy. Lett.* **100** 243101
[10] Rapoport L, Bilik Y, Feldman Y, Homyonfer M, Cohen S R and Tenne R 1997 *Nature* **387** 791
[11] Seifert G, Terrones H, Terrones M, Jungnickel G and Frauenheim T 2000 *Phys. Rev. Lett.* **85** 146
[12] Zibouche N, Kuc A and Heine T 2012 *Eur. Phys. J. B* **85** 49
[13] Ansari R, Malakpour S, Faghihnasiri M and Sahmani S 2015 *Superlattices Microstruct.* **82** 188
[14] Lorenz T, Teich D, Joswig J O and Seifert G 2012 *J. Phys. Chem. C* **116** 11714
[15] Xiao J, Long M, Li X, Xu H, Huang H and Gao Y 2015 *Sci Rep.* **4** 4327
[16] Milošević I, Nikolić B, Dobardžić E, Damnjanović M, Popov I and Seifert G 2007 *Phys. Rev. B* **76** 233414
[17] Tibbetts G G 1984 *J. Cryst. Growth* **66** 632
[18] Seifert G, Köhler T and Tenne R 2002 *J. Phys. Chem. B* **106** 2497
[19] Remškar M, Viršek M and Mrzel A 2009 *Appl. Phy. Lett.* **95** 133122
[20] Lu A Y, Zhu H, Xiao J, Chuu C P, Han Y, Chiu M H, Cheng C C, Yang C W, Wei K H, Yang Y, Wang Y, Sokaras D, Nordlund D, Yang P, Muller D A, Chou M Y, Zhang X and Li L J 2017 *Nat. Nanotech.* **12** 744
[21] Zhang J, Jia S, Kholmanov I, Dong L, Er D, Chen W, Guo H, Jin Z, Shenoy V B, Shi L and Lou J 2017 *ACS Nano* **11** 8192
[22] Zhao W, Li Y, Duan W and Ding F 2015 *Nanoscale* **7** 13586
[23] Wu H H, Meng Q, Huang H, Liu C T and Wang X L 2018 *Phys. Chem. Chem. Phys.* **20** 3608
[24] Bhattacharyya S and Singh A K 2012 *Phys. Rev. B* **86** 075454
[25] Brothers E N, Izmaylov A F, Normand J O, Barone V and Scuseria G E 2008 *J. Chem. Phys.* **129** 011102
[26] Kresse G and Furthmüller J 1996 *Phys. Rev. B* **54** 11169
[27] Blöchl P E 1994 *Phys. Rev. B* **50** 17953
[28] Perdew J P, Burke K and Ernzerhof M 1996 *Phys. Rev. Lett.* **77** 3865
[29] Heyd J, Scuseria G E and Ernzerhof M 2003 *J. Chem. Phys.* **118** 8207
[30] Fuchs F, Furthmüller J, Bechstedt F, Shishkin M and Kresse G 2007 *Phys. Rev. B* **76** 115109
[31] Batsanov S S 2001 *Inorg. Mater.* **37** 871
[32] Ghorbani-Asl M, Zibouche N, Wahiduzzaman M, Oliveira A F, Kuc A and Heine T 2013 *Sci. Rep.* **3** 2961
[33] Zhang Y Y, Du S X and Gao H J 2011 *Phys. Rev. B* **84** 125446